

TGP attenuates endoplasmic reticulum stress and regulates the expression of thioredoxin-interacting protein in the kidneys of diabetic rats

Yunxia Shao¹, Xiangming Qi¹, Xinxing Xu¹, Kun Wang¹, Yonggui Wu^{1,*}, Lingling Xia^{2,*}

¹ Department of Nephropathy, the First Affiliated Hospital of Anhui Medical University, Hefei, Anhui, China;

² Department of Infective Disease, the First Affiliated Hospital of Anhui Medical University, Hefei, Anhui, China.

Summary

Recent evidence suggests that the endoplasmic reticulum stress (ERS)-thioredoxin-interacting protein (TXNIP)-inflammation chain contributes to diabetic renal injury. The aim of the current study was to investigate whether total glucosides of peony (TGP) could inhibit ERS and attenuate up-regulation of TXNIP in the kidneys of rats with streptozotocin-induced diabetes. TGP was orally administered daily at a dose of 50, 100, or 200 mg/kg for 8 weeks. The expression of glucose-regulated protein 78 (GRP78), phospho-protein kinase RNA-like ER kinase (p-PERK), phospho-eukaryotic translation initiation factor 2 α (p-eIF2 α), C/EBP-homologous protein (CHOP), and TXNIP was assessed. Results indicated that TGP significantly decreased diabetes-induced albuminuria and it acted by down-regulating activation of the ERS-TXNIP-inflammation chain in the kidneys of diabetic rats. These findings indicate that renoprotection from TGP in diabetic rats possibly contributed to inhibition of ERS and decreased expression of TXNIP. These findings also offer a new perspective from which to study the molecular mechanisms of diabetic nephropathy and prevent its progression.

Keywords: Diabetic nephropathy, endoplasmic reticulum stress, thioredoxin-interacting protein, total glucosides of peony

1. Introduction

Diabetic nephropathy (DN) is currently prevalent around the world and accounts for nearly one-third of cases of end-stage renal disease. In clinical settings, treatments for DN usually consist of close monitoring of blood glucose and blood pressure and use of medications such as renin-angiotensin system (RAS) blockers. Nonetheless, DN worsens in many patients, increasing the need for dialysis

and eventually leading to organ failure (1,2).

Over the past few years, several studies have indicated that endoplasmic reticulum stress (ERS) plays a crucial role in the pathogenesis of diabetic vascular complications (3,4). An ERS response may be triggered by a stressful stimulus (e.g., hyperglycemia, oxidative stress, albuminuria, advanced glycation end products (AGEs), and activation of RAS (5-8)), that exhausts or disrupts normal protein folding by the endoplasmic reticulum, thus causing accumulation of misfolded and/or unfolded proteins. ERS may also activate the unfolded protein response (UPR) pathway that is initiated by glucose-regulated protein 78 (GRP78) and three endoplasmic reticulum transmembrane sensors - inositol requiring enzyme 1 α (IRE1 α), protein kinase RNA-like ER kinase (PERK), and activating transcription factor 6 (ATF6) (9). Therefore, the overexpression of IRE1 α , PERK, and ATF6 contribute to a modified endoplasmic reticulum or the continued presence of unfolded proteins, resulting in insufficient protein folding.

Inflammation plays a leading role in the pathogenesis

Released online in J-STAGE as advance publication December 24, 2016.

*Address correspondence to:

Dr. Yonggui Wu, Department of Nephropathy, the First Affiliated Hospital of Anhui Medical University, Hefei, Anhui 230022, China.

E-mail: wuyonggui@medmail.com.cn

Dr. Lingling Xia, Department of Infective Disease, the First Affiliated Hospital of Anhui Medical University, Hefei, Anhui 230022, China.

E-mail: wuyongguixialiang@163.com

of DN (10,11). A key molecule, thioredoxin-interacting protein (TXNIP, and also known as vitamin-D3 up-regulated protein-1 (VDUP1) or thioredoxin binding protein-2 (TBP-2)), has been found to link ERS to inflammation and cell death (12,13). ERS can induce TXNIP activation through the PERK and IRE1 pathways, it can provoke interleukin 1 β (IL-1 β) mRNA transcription, and it can mediate ERS-mediated β cell death (13). Microarray studies indicated that the expression of TXNIP mRNA was markedly elevated in human islet cells and renal tubular cells (14,15). More recently, studies have found that TXNIP can induce oxidative stress and increase extracellular matrix production, causing the development of DN (16). Thus, the prevention of TXNIP expression may inhibit the progression of DN (17). Accordingly, the ERS-TXNIP-inflammation chain may be a novel target for DN therapy.

Over the past few years, patients with DN have become increasingly interested in Chinese herbal therapies. The dried root of *Paeonia lactiflora* Pall. is often used in Chinese herbal remedies, where it is commonly referred to as white peony root (baishao in Chinese). Total glucosides of peony (TGP) are active compounds that can be extracted from the dried roots of *Paeonia lactiflora* Pall. Reversed-phase high-performance liquid chromatography (HPLC) has indicated that TGP contain eight principal components, namely paeoniflorin, oxypaeoniflorin, benzoylpaeoniflorin, benzoyloxypaeoniflorin, oxybenzoyl-paeoniflorin, albiflorin, paeoniflorigenone, and lactiflorin (Figure 1 (18)). TGP are considered to have antiinflammatory, antioxidative, hepatoprotective, and immunoregulatory actions (19-21). TGP are a disease-modifying medication for rheumatoid arthritis that was approved by the State Food and Drug Administration (SFDA) in 1998. Recently, TGP have been used to treat chronic nephritis in rats (22), and their action may involve the regulation of the expression of IL-1 and IL-1 α mRNA (23). In previous studies, the current authors experimentally induced DN, and results indicated that TGP prevented inflammation, oxidation, and macrophage activation, thus slowing the progression of DN (24-26). However, the effect of TGP on the ERS-TXNIP-inflammation chain in DN remains unclear. The aim of the current study was to determine how TGP averts renal injury in diabetic rats in terms of the ERS-TXNIP-inflammation chain.

2. Materials and Methods

2.1. Reagents

TGP was extracted from the roots of *P. lactiflora* Pall. using ethanol reflux, n-butanol extraction, and macroreticular absorption resin chromatography. HPLC fingerprinting analysis indicated that the

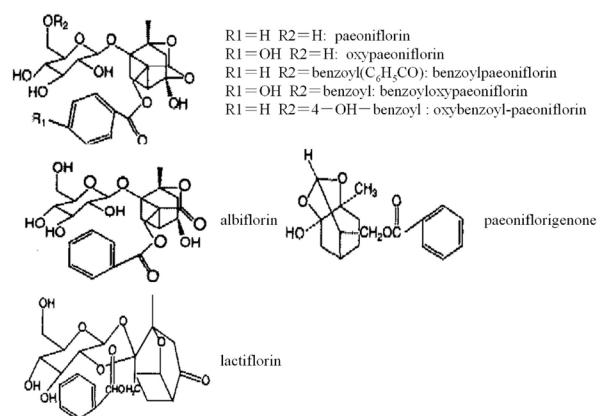


Figure 1. Chemical structures of the major components of total glucosides of peony.

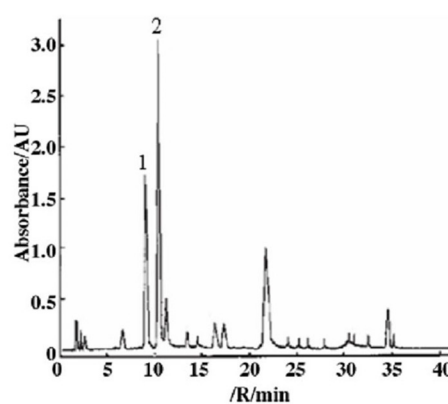


Figure 2. HPLC fingerprinting of total glucosides of peony. (1) Albiflorin; (2) Paeoniflorin. Column: Supelcosil LC-18 (5 mm, 150 mm \times 4.6 mm); Solvent A: Acetonitrile; Solvent B: H₂O (acidified to pH 3.0 with phosphoric acid); Gradient: 10%, 15%, 18%, 30%, 35%, 40%. And 40% of solvent A at 0, 5, 25, 27, 38, 40, and 50 min, respectively. Flow rate: 1.0 mL/min. Injection volume: 10 mL. Detection: 230 nm.

extract contained 41.1% paeoniflorin (Figure 2) (27). Streptozotocin (STZ) was obtained from Sigma Chemical Co. (St. Louis, MO, USA). A microalbumin assay kit was purchased from Abcam Biotechnology (Abcam, Cambridge, UK). An immunohistochemistry kit (PV-9000) was purchased from Beijing Zhongshan Biotechnology, Inc. (Zhongshan, China). TXNIP and a GAPDH primer were obtained from Shanghai Sangon Co. (Shanghai, China). A Trizol Kit was obtained from Invitrogen (Invitrogen, California, USA). M-MLV reverse transcriptase and an RNA enzyme inhibitor were purchased from Promega (Madison, WI, USA). A SYBR Green PCR Master Mix Kit was obtained from Bio-Rad Laboratories (Hercules, CA, USA). The following antibodies were used in this study: rabbit anti-GRP78 and anti-TXNIP antibodies were obtained from Santa Cruz Biotechnology (Santa Cruz, CA, USA), and anti-p-PERK, anti-p-eIF2 α , and anti-CHOP antibodies were purchased from Cell Signaling (USA). Anti- β -actin antibodies, anti-rabbit IgG, and anti-mouse IgG antibodies conjugated to horseradish peroxidase (HRP)

were purchased from Wuhan Sanying Biotechnology, Inc. (Wuhan, China). A bicinchoninic acid (BCA) kit was obtained from Beyotime Institute of Biotechnology (Jiangsu, China). A chemiluminescence kit was obtained from Amersham Life Science (Little Chalfont, UK).

2.2. Animals

Male Munich-Wistar rats ($n = 50$, weight: 180 to 200 g) were purchased from the Experimental Animal Center of Anhui Medical University. Each cage contained 5 animals with free access to food and water. Animals were housed in a constant environment (temperature of about $24 \pm 1^\circ\text{C}$, 60% humidity, 12:12-h light:dark cycle). This study was approved by the Animal Ethics Committees of the Faculty of Anhui Medical University and animals were treated in accordance with the "Principles of Laboratory Animal Care and Use in Research" (Ministry of Health, Beijing, China).

2.3. Experimental design

After ten days of acclimation, rats fasted overnight and were then injected with 65 mg/kg of streptozotocin in a citrate buffer (0.1 M, pH 4.5) based on their weight. Two days later, blood glucose and body weight were evaluated and only rats with blood glucose levels higher than 16.8 mmol/L were used in this study. Diabetic rats were randomly divided into four groups (a diabetic control group and TGP intervention groups) with no differences among the groups. TGP intervention groups were administered TGP daily at a dose of 50, 100, or 200 mg/kg *via* a stomach tube, while the non-diabetic control group and diabetic control group were administered an equivalent amount of 0.5% sodium carboxymethylcellulose (CMC-Na).

2.4. Urinary albumin excretion

Prior to sacrifice, 24-h urine samples were collected from rats housed in metabolic cages in order to measurement urinary albumin excretion. Samples were centrifuged at 10,000 g for 3 min at 4°C and final volumes were recorded. Albumin levels were detected using the Rat Albumin ELISA Kit in accordance with the manufacturer's instructions.

2.5. Blood samples and tissue collection

After 8 wk of follow-up, rats fasted 12 h, and 10 rats from each group were euthanized by intraperitoneal injection of sodium pentobarbital (50 mg/kg). Blood samples were immediately collected by catheterizing the right jugular artery and then the rats were perfused with normal saline at 4°C . After the rats were perfused, one kidney was fixed in a 10% formaldehyde solution for immunohistochemical experiments and another kidney

was stored at -80°C for further analysis.

2.6. Immunohistochemistry

Immunoperoxidase staining for GRP78 was performed on 10% formalin-fixed paraffin sections (2 μm). Three-percent hydrogen peroxide was used to block endogenous peroxidase and antigens were retrieved with microwave heating. Tissue sections were blocked with 10% normal goat serum for 10 min followed by incubation with anti-GRP78 antibodies (1:100) overnight at 4°C . The sections were washed in phosphate-buffered saline and incubated with the appropriate horseradish peroxidase-labeled secondary antibody for 30 min at 37°C . After sections were rinsed, reactions were visualized using 3,3-diaminobenzidine (DAB, Sigma), with a brown color indicating peroxidase activity. Sections were counterstained with hematoxylin. Immunostaining of GRP78 was evaluated using the Image-Pro Plus 6.0 image analysis system by quantifying the stained area of the sections and the entire field of view at the same light intensity used in microscopy (28). Five fields were randomly selected from each section for observation at a high magnification and the ratio of the stained area to the entire field was calculated.

2.7. Western blot analysis

Tissue samples from each of the 5 groups were homogenized in radio immunoprecipitation assay (RIPA) lysis buffer, and Western blot analysis was performed as described previously (26). Nitrocellulose membranes were blocked with 5% non-fat milk for 2 h and then incubated with the primary antibody at 4°C overnight. Membranes were then treated with horseradish peroxidase-labeled secondary antibody. Blots were developed with enhanced chemiluminescence. The signal intensity of each band was quantified and analyzed using the Leica Q500IW image analysis system, and the result was expressed as a ratio of GRP78, p-PERK, p-eIF2 α , CHOP, and TXNIP to housekeeping protein-actin in optical density units.

2.8. RNA extraction and real-time PCR

Total RNA was extracted from kidney tissue with the Trizol reagent in accordance with the manufacturer's instruction. Real-time PCR was performed using the SYBR Green PCR master mix kit as previously described (26). The primers used in this study were as follows: TXNIP, 5'-TCAGTCAGAGGCAATCACATTA-3', and 5'-GGAGCCAGGGACACTAACATAG-3 and GAPDH, 5'-ACAGCAACAGGGTGGTGGAC-3', and 5'-TTTGAGGGTGCAGCGAACTT-3'. The relative expression of mRNA was analyzed using $2^{-\Delta\Delta\text{Ct}}$, and expression of the mRNA of interest was normalized to GAPDH.

Table 1. Characteristics of the rats clinical and metabolic parameters

Groups	Dose (mg/kg*d)	Blood glucose (mg/dL)	Body weight (g)	Kidney weight/ body weight (g/100g BW)	Albumin excretion rate ^a (mg/24 h)
Normal		123.53 ± 29.19	458 ± 27.47	0.30 ± 0.04	0.38 ×/÷ 1.3
Diabetic control		469.07 ± 74.58**	271.75 ± 16.86**	0.56 ± 0.05*	1.87 ×/÷ 1.1**
Diabetic + TGP	50	445.04 ± 77.43	281.75 ± 25.01	0.52 ± 0.02	1.32 ×/÷ 1.1 [#]
	100	470.49 ± 75.47	266.4 ± 27.87	0.50 ± 0.06	1.15 ×/÷ 1.1 [#]
	200	484.16 ± 75.65	318.0 ± 17.8	0.50 ± 0.04	0.65 ×/÷ 1.1 ^{###}

Data are expressed as means ± S.E.M. ^aShown as geometric mean ×/÷ tolerance factor. Number of rats in each group was 10. **p* < 0.05, ***p* < 0.01, compared with normal group; [#]*p* < 0.05, ^{###}*p* < 0.01 compared with diabetic control group.

2.9. Statistical analysis

Data obtained from this study are expressed as the mean ± S.E.M. unless otherwise specified. For statistical analysis, ANOVA was performed using SPSS 16.0. The difference between groups was tested using the LSD test and Levene's test for homogeneity of variance, where *p* < 0.05 was considered to indicate a significant difference. Since the rate of urinary albumin excretion followed a skewed distribution, log transformation was used prior to statistical analysis of this parameter.

3. Results

3.1. TGP attenuated an increase in albuminuria in diabetic rats

TGP treatment did not cause any significant changes in body weight, blood glucose levels, and the ratio of the kidney weight to body weight among the diabetic groups. Accumulated evidence has indicated that albuminuria is a leading risk factor for the progression of renal disease (29,30). TGP significantly attenuated the high level of albuminuria in all of the diabetic groups (Table 1). Although that attenuation was dose-dependent, the levels of albuminuria were still higher than those in normal control rats. This finding suggests that TGP can potentially protect the kidneys and prevent the development of DN.

3.2. TGP inhibited the expression of GRP78 in the kidneys of rats with STZ-induced diabetes

GRP78 is a marker of ERS and has been implicated in the pathogenesis of diabetic complications (9). GRP78 was noted in the glomerulus and tubulointerstitium. There was minimal staining for GRP78 in the kidneys of normal rats, while GRP78 was abundantly expressed in the kidneys of diabetic rats. Overexpression of GRP78 was more limited in diabetic rats treated with TGP (Figure 3 and Table 2). Densitometric analysis of Western blots revealed that the level of GRP78 protein was markedly higher in control diabetic rats than in normal rats. As shown in Figure 4, TGP at a dose of 50, 100, or 200 mg/kg significantly down-regulated renal expression of GRP78 protein in diabetic rats according

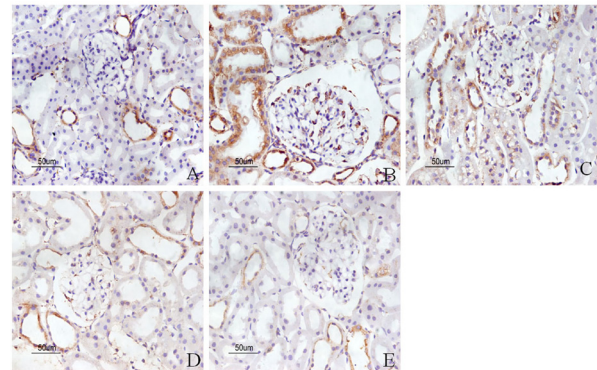


Figure 3. Immunostaining of GRP78 in the kidney. (A) normal; (B) control diabetic; (C) diabetic + TGP 50 mg/kg; (D) diabetic + TGP 100 mg/kg; (E) diabetic + TGP 200 mg/kg. Original magnification ×400.

Table 2. Semiquantitative assessment of GRP78 immunohistochemistry staining in five groups of rats

Groups	Dose (mg/kg*d)	Glomeruli (%) ^a	Tubulointerstitium (%) ^a
Normal		0.75 ± 0.53	5.05 ± 0.77
Diabetic control		12.42 ± 5.56**	18.93 ± 1.67**
Diabetic + TGP	50	9.46 ± 1.83 [#]	15.60 ± 2.07 ^{##}
	100	5.79 ± 1.89 ^{###}	12.33 ± 3.46 ^{###}
	200	4.89 ± 2.26 ^{###}	10.25 ± 3.27 ^{###}

Data are expressed as means ± S.E.M. ^aShown as the median. Number of rats in each group was 10. ***p* < 0.01, compared with the normal group; [#]*p* < 0.05, ^{###}*p* < 0.01, compared with the control diabetic group.

to Western blot analysis.

3.3. TGP reduced the expression of p-PERK and p-eIF2α in the kidneys of rats with STZ-induced diabetes

ERS caused abnormal levels of p-PERK and p-eIF2α expression. As indicated by densitometric analysis of Western blots, the levels of p-PERK and p-eIF2α expression were significantly higher in diabetic rats than in normal rats. However, TGP treatment caused the levels of p-PERK and p-eIF2α expression to decrease markedly (Figure 4).

3.4. TGP attenuated the expression of CHOP in the kidneys of rats with STZ-induced diabetes

CHOP (or GADD153) is an integral component of

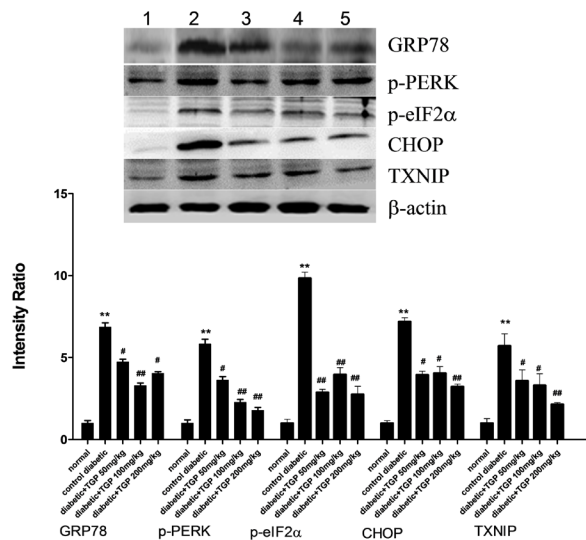


Figure 4. Western blot analysis of GRP78, p-PERK, p-eIF2 α , CHOP, and TXNIP in renal tissue from five groups of rats. (1) normal; (2) control diabetic; (3) diabetic + TGP 50 mg/kg; (4) diabetic + TGP 100 mg/kg; (5) diabetic + TGP 200 mg/kg. Densitometric data were normalized to β -actin levels and values for each control group were arbitrarily defined as 1. Results are expressed as the mean \pm S.E.M from at least three independent experiments. ** $p < 0.01$ vs. normal, # $p < 0.05$, ## $p < 0.01$ vs. control diabetic.

ERS-induced apoptosis; importantly, CHOP is also a component of the inflammatory response (10). In order to investigate whether TGP was involved in the pathogenesis of DN *via* the inflammatory response, the level of CHOP expression was determined using Western blot analysis. The level of CHOP protein was markedly higher in control diabetic rats than in normal rats. Like the findings mentioned earlier, the activation of CHOP diminished dramatically as a result of treatment with TGP at a dose of 50, 100, or 200 mg/kg (Figure 4).

3.5. TGP attenuated the expression of TXNIP in the kidneys of rats with STZ-induced diabetes

The current study focused on TXNIP, which is an important link between ERS and inflammation (12,13). The current results indicated that TXNIP tended to increase in rats with STZ-induced diabetes. As shown in Figure 4, the level of TXNIP expression decreased markedly with administration of TGP at a dose of 50, 100, or 200 mg/kg. The level of TXNIP mRNA expression in the renal tissues of rats with DN was significantly higher than that in the control group, and that level of expression decreased markedly as a result of treatment with TGP (Figure 5).

4. Discussion

Previous studies by the current authors indicated that the weight of the kidney, the glomerular volume, the tubulointerstitial damage index, and the rate of urinary albumin excretion improved markedly 8 weeks

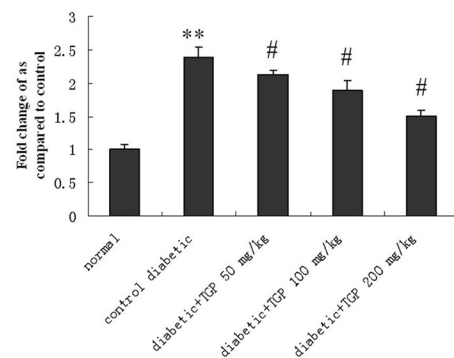


Figure 5. Quantitative real-time PCR of TXNIP in the kidney. Values are expressed as the mean \pm S.E.M from at least three independent experiments. ** $p < 0.01$ vs. normal, # $p < 0.05$ vs. control diabetic.

after diabetes was induced with STZ; however, TGP ameliorated albuminuria and it attenuated glomerular and tubulointerstitial injuries without changing blood glucose levels (24,25,31). This suggested that TGP might prove to be a useful therapy for DN. The current results suggested that type 1 diabetes mellitus induced with STZ was associated with activation of the renal ERS response and upregulation of TXNIP. Previous studies have indicated that the protective effects of TGP in diabetic rats were related to its antiinflammatory and antioxidative action. The current study further identified the effects of TGP on ERS and TXNIP in diabetic rats.

Diabetes has been characterized as a chronic inflammatory disease (31,32) and is associated with abnormal secretion of numerous inflammatory factors. The increased UPR in diabetes reveals the existence of ERS (33), including upregulation of nuclear transcription factors such as PERK. Fang *et al.* reported that ERS appeared to play an important part in albuminuria-provoked inflammasome activation and elimination of ERS *via* tauroursodeoxycholic acid (TUDCA), which might represent a novel avenue for attenuating kidney epithelial cell damage caused by albuminuria (34). The UPR is a homeostatic response that allows the cells to cope with stressful conditions associated with increased misfolded or unfolded protein loads; failure of this mechanism is referred to as the ERS response (9). The ERS response has been found to play a key role in a growing number of pathological conditions such as DN (10,34,35), and the ERS response is considered to be a cause of chronic inflammation (36). The current results verified the hypothesis that DN is related to ERS *via* dysregulated expression of GRP78, p-PERK, p-eIF2 α , and CHOP.

Recent experimental evidence suggests that TXNIP occupies a critical node in signaling that connects ERS and IL-1 β production. TXNIP expression was induced by ERS *via* the IRE1 α and PERK-eIF2 α pathways of the UPR. Carbohydrate response element binding protein (ChREBP) and activating transcription factor 5 (ATF5) regulate TXNIP expression at the

transcriptional level (12,13), while IRE1 α regulates TXNIP expression at the posttranscriptional level (12). Consequently, cell death is induced by IL-1 β production caused by TXNIP through the initiation of IL-1 β mRNA transcription. Transcriptional activation of IL-1 β might explain the upregulation of TXNIP caused by ERS (37). TXNIP is also considered to be as a crucial signaling molecule that connects oxidative stress and inflammasome activation (38). Studies of endothelial cells have indicated that activation of the ERS-TXNIP-inflammation chain was responsible for endothelial dysfunction (39,40). Suppressing ERS, regulating TXNIP expression, and inhibiting inflammation have proven beneficial in the management of cardiovascular disease in obese individuals and diabetics (39,41).

TGP are isolated from the roots of *P. lactiflora* Pall. and are used in clinical settings to alleviate an inflammatory reaction. The roots of *P. lactiflora* Pall. have long been used as a treatment for rheumatoid arthritis. Recent studies in China had reported that TGP cure nephritis, including Heymann nephritis and IgA nephropathy. Together with previous results indicating that TGP treatment reduces the expression of tumor necrosis factor α (TNF- α) and IL-1 β (26), the current results indicated that TXNIP might be a critical hub between ERS and IL-1 β . Numerous stress signaling pathways may converge at TXNIP, contributing to inflammasome activation and pro-inflammatory cytokine production. An important finding is that TGP may inhibit the upregulation of TXNIP and ERS in diabetic kidneys *via* the attenuation of pro-inflammatory cytokine production. Therefore, TGP could possibly play a pivotal role in the treatment of DN.

Together with the results of recent studies, the current findings indicated that there are close ties among ERS, glucose toxicity, oxidative stress, and inflammation in DN, suggesting that a therapeutic strategy targeting TXNIP might be effective in treating DN. However, the specific mechanism by which TGP acts on ERS and TXNIP is not yet fully understood. This topic will be examined in further studies in the future.

Acknowledgements

This research was funded by the National Natural Science Foundation of China (No. 81374034) and the Natural Science Foundation of Anhui Province (No.1408085MH183, No.1208085MH149).

References

1. Grace BS, Clayton P, McDonald SP. Increases in renal replacement therapy in Australia and New Zealand: Understanding trends in diabetic nephropathy. *Nephrology*. 2012; 17:76-84.
2. Taler SJ, Agarwal R, Bakris GL, Flynn JT, Nilsson PM, Rahman M, Sanders PW, Textor SC, Weir MR, Townsend RR. KDOQI US commentary on the 2012 KDIGO clinical

- practice guideline for management of blood pressure in CKD. *Am J Kidney Dis*. 2013; 62:201-213.
3. Khan MI, Pichna BA, Shi Y, Bowes AJ, Werstuck GH. Evidence supporting a role for endoplasmic reticulum stress in the development of atherosclerosis in a hyperglycaemic mouse model. *Antioxid Redox Signal*. 2009; 11:2289-2298.
4. Chen Y, Wang JJ, Li J, Hosoya KI, Ratan R, Townes T, Zhang SX. Activating transcription factor 4 mediates hyperglycaemia-induced endothelial inflammation and retinal vascular leakage through activation of STAT3 in a mouse model of type 1 diabetes. *Diabetologia*. 2012; 55:2533-2545.
5. Lindenmeyer MT, Rastaldi MP, Ikehata M, Neusser MA, Kretzler M, Cohen CD, Schlondorff D. Proteinuria and hyperglycemia induce endoplasmic reticulum stress. *J Am Soc Nephrol*. 2008; 19:2225-2236.
6. Liu G, Sun Y, Li Z, Song T, Wang H, Zhang Y, Ge Z. Apoptosis induced by endoplasmic reticulum stress involved in diabetic kidney disease. *Biochem Biophys Res Commun*. 2008; 370:651-656.
7. Inagi R, Nangaku M, Onogi H, Ueyama H, Kitao Y, Nakazato K, Ogawa S, Kurokawa K, Couser WG, Miyata T. Involvement of endoplasmic reticulum (ER) stress in podocyte injury induced by excessive protein accumulation. *Kidney Int*. 2005; 68:2639-2650.
8. Liu J, Huang K, Cai GY, Chen XM, Yang JR, Lin LR, Yang J, Huo BG, Zhan J, He YN. Receptor for advanced glycation end-products promotes premature senescence of proximal tubular epithelial cells *via* activation of endoplasmic reticulum stress-dependent p21 signaling. *Cell Signal*. 2014; 26:110-121.
9. Kitamura M. Endoplasmic reticulum stress in the kidney. *Clin Exp Nephrol*. 2008; 12:317-325.
10. Wu J, Zhang R, Torreggiani M, Ting A, Xiong H, Striker GE, Vlassara H, Zheng F. Induction of diabetes in aged C57B6 mice results in severe nephropathy: An association with oxidative stress, endoplasmic reticulum stress, and inflammation. *Am J Pathol*. 2010; 176:2163-2176.
11. Saraheimo M, Teppo AM, Forsblom C, Fagerudd J, Groop PH. Diabetic nephropathy is associated with low-grade inflammation in Type 1 diabetic patients. *Diabetologia*. 2003; 46:1402-1407.
12. Lerner AG, Upton JP, Praveen PV, *et al*. IRE1 α induces thioredoxin-interacting protein to activate the NLRP3 inflammasome and promote programmed cell death under irremediable ER stress. *Cell Metab*. 2012; 16:250-264.
13. Osowski CM, Hara T, O'Sullivan-Murphy B, Kanekura K, Lu S, Hara M, Ishigaki S, Zhu LJ, Hayashi E, Hui ST, Greiner D, Kaufman RJ, Bortell R, Urano F. Thioredoxin-interacting protein mediates ER stress-induced beta cell death through initiation of the inflammasome. *Cell Metab*. 2012; 16:265-273.
14. Shalev A, Pise-Masison CA, Radonovich M, Hoffmann SC, Hirshberg B, Brady JN, Harlan DM. Oligonucleotide microarray analysis of intact human pancreatic islets: Identification of glucose-responsive genes and a highly regulated TGF beta signaling pathway. *Endocrinology*. 2002; 143:3695-3698.
15. Qi W, Chen X, Gilbert RE, Zhang Y, Waltham M, Schache M, Kelly DJ, Pollock CA. High glucose-induced thioredoxin-interacting protein in renal proximal tubule cells is independent of transforming growth factor-beta1. *Am J Pathol*. 2007; 171:744-754.

16. Advani A, Gilbert RE, Thai K, *et al.* Expression, localization, and function of the thioredoxin system in diabetic nephropathy. *J Am Soc Nephrol.* 2009; 20:730-741.
17. Hamada Y, Fukagawa M. A possible role of thioredoxin interacting protein in the pathogenesis of streptozotocin-induced diabetic nephropathy. *Kobe J Med Sci.* 2007; 53:53-61.
18. Li J, Chen CX, Shen YH. Effects of total glucosides from paeony (*Paeonia lactiflora* Pall) roots on experimental atherosclerosis in rats. *J Ethnopharmacol.* 2011; 135:469-475.
19. Wang Y, Zhang H, Du G, Wang Y, Cao T, Luo Q, Chen J, Chen F, Tang G. Total glucosides of paeony (TGP) inhibits the production of inflammatory cytokines in oral lichen planus by suppressing the NF-kappaB signaling pathway. *Int Immunopharmacol.* 2016; 36:67-72.
20. Zhang LL, Wei W, Wang NP, Wang QT, Chen JY, Chen Y, Wu H, Hu XY. Paeoniflorin suppresses inflammatory mediator production and regulates G protein-coupled signaling in fibroblast-like synoviocytes of collagen induced arthritic rats. *Inflamm Res.* 2008; 57:388-395.
21. Liu DF, Wei W, Song LH. Protective effect of paeoniflorin on immunological liver injury induced by bacillus Calmette-Guerin plus lipopolysaccharide: Modulation of tumour necrosis factor-alpha and interleukin-6 mRNA. *Clin Exp Pharmacol Physiol.* 2006; 33:332-339.
22. Zhou DY, Xu XM, Dai H, Feng J. Effect of total glucosides of paeony on mesangial proliferative glomerulonephritis in rats. *Acta Universitatis Medicinalis Anhui.* 2006; 41:146-149. (in Chinese)
23. Zhang MO, Wang YW, Zhu XL, Yang RC, Zhang YH, Lu Y, Wang YJ. Total glucosides of peony reduces renal damage in rats with mesangial proliferative nephritis. *Zhe Jiang Medical Journal.* 2008; 30:1176-1179. (in Chinese)
24. Su J, Zhang P, Zhang JJ, Qi XM, Wu YG, Shen JJ. Effects of total glucosides of paeony on oxidative stress in the kidney from diabetic rats. *Phytomedicine.* 2010; 17:254-260.
25. Wang K, Wu YG, Su J, Zhang JJ, Zhang P, Qi XM. Total glucosides of paeony regulates JAK2/STAT3 activation and macrophage proliferation in diabetic rat kidneys. *Am J Chin Med.* 2012; 40:521-536.
26. Xu XX, Qi XM, Zhang W, Zhang CQ, Wu XX, Wu YG, Wang K, Shen JJ. Effects of total glucosides of paeony on immune regulatory toll-like receptors TLR2 and 4 in the kidney from diabetic rats. *Phytomedicine.* 2014; 21:815-823.
27. Zou ZM, Li-Zhen XU, Yang SL. HPLC fingerprinting of total glucosides of paeony. *Acta Pharmaceutica Sinica.* 2003; 38:46-49. (in Chinese)
28. Aoyama I, Shimokata K, Niwa T. An oral adsorbent downregulates renal expression of genes that promote interstitial inflammation and fibrosis in diabetic rats. *Nephron.* 2002; 92:635-651.
29. Bakris GL. Slowing nephropathy progression: Focus on proteinuria reduction. *Clin J Am Soc Nephrol.* 2008; 3 Suppl 1:S3-10.
30. de Zeeuw D, Remuzzi G, Parving HH, Keane WF, Zhang Z, Shahinfar S, Snapinn S, Cooper ME, Mitch WE, Brenner BM. Proteinuria, a target for renoprotection in patients with type 2 diabetic nephropathy: Lessons from RENAAL. *Kidney Int.* 2004; 65:2309-2320.
31. Wu Y, Ren K, Liang C, Yuan L, Qi X, Dong J, Shen J, Lin S. Renoprotective effect of total glucosides of paeony (TGP) and its mechanism in experimental diabetes. *J Pharmacol Sci.* 2009; 109:78-87.
32. Li J, Wang JJ, Yu Q, Wang M, Zhang SX. Endoplasmic reticulum stress is implicated in retinal inflammation and diabetic retinopathy. *FEBS Lett.* 2009; 583:1521-1527.
33. Hotamisligil GS. Endoplasmic reticulum stress and the inflammatory basis of metabolic disease. *Cell.* 2010; 140:900-917.
34. Fang L, Xie D, Wu X, Cao H, Su W, Yang J. Involvement of endoplasmic reticulum stress in albuminuria induced inflammasome activation in renal proximal tubular cells. *PLoS one.* 2013; 8:e72344.
35. Baban B, Liu JY, Mozaffari MS. Endoplasmic reticulum stress response and inflammatory cytokines in type 2 diabetic nephropathy: Role of indoleamine 2,3-dioxygenase and programmed death-1. *Exp Mol Pathol.* 2013; 94:343-351.
36. Hasnain SZ, Lourie R, Das I, Chen AC, McGuckin MA. The interplay between endoplasmic reticulum stress and inflammation. *Immunol Cell Biol.* 2012; 90:260-270.
37. Koenen TB, Stienstra R, van Tits LJ, de Graaf J, Stalenoef AF, Joosten LA, Tack CJ, Netea MG. Hyperglycemia activates caspase-1 and TXNIP-mediated IL-1beta transcription in human adipose tissue. *Diabetes.* 2011; 60:517-524.
38. Zhou R, Tardivel A, Thorens B, Choi I, Tschopp J. Thioredoxin-interacting protein links oxidative stress to inflammasome activation. *Nat Immunol.* 2010; 11:136-140.
39. Li Y, Yang J, Chen MH, Wang Q, Qin MJ, Zhang T, Chen XQ, Liu BL, Wen XD. Ilexgenin A inhibits endoplasmic reticulum stress and ameliorates endothelial dysfunction via suppression of TXNIP/NLRP3 inflammasome activation in an AMPK dependent manner. *Pharmacol Res.* 2015; 99:101-105.
40. Zhao Y, Li Q, Zhao WJ, Li J, Sun Y, Liu K, Liu BL, Zhang N. Astragaloside IV and cycloastragenol are equally effective in inhibition of endoplasmic reticulum stress-associated TXNIP/NLRP3 inflammasome activation in the endothelium. *J Ethnopharmacol.* 2015; 169:210-218.
41. Song JN, Li J, Hou FJ, Wang XN, Liu BL. Mangiferin inhibits endoplasmic reticulum stress-associated thioredoxin-interacting protein/NLRP3 inflammasome activation with regulation of AMPK in endothelial cells. *Metabolism.* 2014; 64:428-437.

(Received October 14, 2016; Revised November 30, 2016; Accepted December 4, 2016)